CHEMISTRY
A EUROPEAN JOURNAL

Supporting Information

Supramolecular Helical Fluid Columns from Self-Assembly of Homomeric Dipeptides

Channabasaveshwar V. Yelamaggad[a]*, Govindaswamy Shanker[a], R. V. Ramana Rao[b] Doddamane S. Shankar Rao[a], Subbarao Krishna Prasad[a], Vommina V. Suresh Babu[b]

[a]*Centre for Liquid Crystal Research*

Jalahalli, Bangalore 560 013, INDIA

Fax: 91-80-28382044

[b]*Department of Studies in Chemistry*

Central College Campus, Bangalore University

Bangalore 560 001, INDIA

Contents

I. General

The requisite starting materials were obtained from either from Aldrich or Lancaster Company and used as received. All the solvents were purified and dried by standard methods prior to use. The crude samples were purified by column chromatographic technique using either silica gel (400 mesh) or neutral aluminium oxide as a stationary phase. Thin layer chromatography (TLC) was performed on aluminium sheets pre-coated with silica gel (Merck, Kieselgel 60, F_{254}). The absorption spectra were recorded on a Perkin-Elmer Lambda 20 UV-Vis spectrometer. IR spectra were recorded using Perkin

Elmer Spectrum 1000 FT-IR spectrometer. ^{1}H NMR spectra were recorded using either a Bruker AMX-400 (400 MHz) or a Bruker Aveance series DPX-200 (200MHz) spectrometer and the chemical shifts are reported in parts per million (ppm) relative to tetramethylsilane (TMS) as an internal standard. Mass spectra were recorded on a Jeol-JMS-600H spectrometer in FAB^+ mode using 3-nitrobenzyl alcohol as a liquid matrix. Elemental analyses were done using Eurovector model EA 3000 CHNS analyzer. The specific rotation of the target molecules was measured using a JASCO DIP-370 digital polarimeter. CD spectrums were recorded with the aid of Jasco J-810 spectropolorimeter. The identification of the mesophases and the transition temperatures of the compounds were initially determined using a polarizing microscope (Leitz DMRXP) in conjunction with a programmable hot stage (Mettler FP90). The transition temperatures and associated enthalpies were determined by differential scanning calorimetry (Perkin Elmer DSC7). X-Ray diffraction studies were carried on powder samples in Lindemann capillaries with CuK_α radiation using an Image Plate Detector (MAC Science, Japan) equipped with a double mirror focusing optics. Nova 600 NanoSEM, high-resolution field emission-SEM column with monopole magnetic immersion final lens, 60 degree objective lens geometry, heated objective aperatures and through-the-lens differential pumping.

II. Experimental

General procedure for the synthesis of compounds: **17**, **18**, **19a**, **19b**, **20a** and **20b**

To an ice-cold solution of Fmoc-amino acid **27a-28b** (1 mmol) in dry THF (5 ml) *N*-methylmorpholine (NMM) (0.11 ml, 1 mmol) and IBC-Cl (0.135 ml, 1 mmol) were added and stirred for 10 min. Trialkoxyaniline (1 mmol) in dry THF was added in one lot to the reaction mixture at the same temperature and stirring continued overnight. The reaction mixture was concentrated and the residue obtained was dissolved in CH_2Cl_2 (20 ml). It was washed successively twice with 5% HCl, 5% aq $NaHCO_3$, brine and dried over anhydrous Na_2SO_4. Evaporation of the solvent in *vacuo* and recrystallisation of the resulting residue using ethanol yielded the product as a white amorphous solid. The product was used in the next step without any further purification.

General procedure for the synthesis of compounds: **13**, **14**, **15a**-**b**,**16a-b**, **5**, **6**, **7a-c** and **8a**-**c**

N^{α}-Fmoc-amino acid amide **17**-**20b** (1 mol) in CH_2Cl_2 (5 ml) was treated with diethyl amine (5 ml) under nitrogen atmosphere until TLC analysis indicated the complete disappearance of the starting material. The solution was concentrate in vacuo, and the residue was further dried in vacuo for an hour. It was utilized for the coupling reaction without any further purification.

General procedure for the synthesis of compounds: **9**, **10**, **11a**-**c** and **12a-c**

To an ice-cold stirred solution of Fmoc-amino acid (1 mmol) in dry THF (5 ml) NMM (0.11 ml, 1 mmol) and IBC-Cl (0.135 ml, 1 mmol) stirred for 10 min., amino acid amide **13-16b** (1 mmole) in dry THF was added at the same temperature and stirring continued overnight. The reaction mixture was concentrated and the residue was dissolved in CH_2Cl_2 (20 ml). It was washed successively twice using 5% HCl, 5% aq $NaHCO_3$, brine and dried over anhydrous Na_2SO_4. Evaporation of the solvent in vacuo and recrystallisation of the resulting residue using ethanol yielded the product as an amorphous white solid. It was utilized directly in the next step.

General procedure for the synthesis of the target compounds: **1**, **2**, **3a-c** and **4a-c**

To the alkoxybenzoic acid (1 mmol) dissolved in THF (10 ml) was added DIEA (0.16 ml, 1.1 mmole), HBTU (0.468 g, 1 mol) and dipeptide amide **5-8c** (1 mol, obtained by the deportation of Fmoc group from **9-12c**) in THF (10 ml) at room temperature and stirred overnight, The reaction mixture was concentrated under reduced pressure and the residue was dissolved in CH_2Cl_2 (20 ml), washed successively twice using 5% HCl, 5% aq $NaHCO_3$, brine and dried over anhydrous Na_2SO_4. Evaporation of the solvent and recrystallization of the resulting residue using ethanol yielded the product as an amorphous white solid.

1 : R_f = 0.67 in 20% EtOAc-hexanes; yield: 70%; IR (KBr pellet): ν = 3273, 2922, 2865, 1628, 1580 cm^{-1}; $[\alpha]_D^{24}$ = -8.6 (c = 1 in $CHCl_3$); UV/Vis: λ_{max} = 269.38 nm, $\in$ = 0.21 × 10^3 L $mol^{-1}cm^{-1}$; ^{1}H NMR (400MHz, $CDCl_3$): δ 8.22 (s, 1H, NH), 7.74 (d, J = 8.8, 2H, Ar), 7.49 (d, J = 8.8, 2H, Ar), 6.93 (d, J =

8.8, 2H, Ar), 6.85 (d, J = 9.2, 2H, Ar), 6.7 (d, J = 6.6, 1H, NH), 6.40 (d, J = 5.4, 1H, NH), 4.65 (m, 1H, CH), 4.55 (m, 1H, CH), 3.99 – 3.91 (t, 4H, OCH_2 × 2), 1.80 – 0.87 (m, 56H, 2 × CH, 18 × CH_2, 6 × CH_3); MS (FAB^+): *m/z* calcd. for $C_{45}H_{74}N_3O_5$ [M^+]: 736.6; found: 736.5; elemental anaylsis calcd (%) for $C_{45}H_{73}N_3O_9$: C 73.43, H 10.0, N 5.71; found: C 73.23, H 9.98, N 5.69.

2 R_f = 0.74 in 20% EtOAc-hexanes; yield: 74%; IR (KBr pellet): ν = 3289, 2923, 2853, 1633, 1612 cm^{-1}; $[\alpha]_D^{24}$ = -2.0 (c = 1 in $CHCl_3$); UV/Vis: λ_{max} = 260.6 nm, ∈ = 2.97 × 10^3 L $mol^{-1}cm^{-1}$; ^{1}H NMR (400MHz, CDCl3): δ 8.30 (s, 1H, NH), 7.26 (d, J = 2.4, 3H, Ar), 6.9 (d, J = 6.6, 1H, NH), 6.81 (d, J = 8.4, 3H, Ar), 6.49 (d, J = 5.4, 1H, NH), 4.25 (m, 1H, CH), 4.15 (m, 1H, CH), 4.03 – 3.93 (m, 8H, OCH_2 × 4), 1.84 – 0.85 (m, 94H, 2 × CH, 34 × CH_2, 8 × CH_3); MS (FAB^+): *m/z* calcd. for $C_{65}H_{114}N_3O_7$[M^+]: 1048.7; found: 1048.3; elemental anaylsis calcd (%) for $C_{65}H_{113}N_3O_7$: C 74.45, H 10.86, N 4.01; found: C 74.23, H 10.78, N, 4.00.

3a : R_f = 0.72 in 40% EtOAc-hexanes; yield: 65%; IR (KBr pellet): ν = 3272, 2923, 2852, 1628, 1600, 1505 cm^{-1}; $[\alpha]_D^{25}$ = -18.75 (c = 1 in $CHCl_3$); UV/VIS: λ_{max} = 263.99 nm, ∈ = 22.69 × 10^3 L $mol^{-1}cm^{-1}$; ^{1}H NMR (400MHz, $CDCl_3$): δ 8.21 (s, 1H, NH), 6.96 (s, 2H, Ar), 6.89 (s, 2H, Ar), 6.75 (d, J = 6.2, 1H, NH), 6.51 (d, J = 6.4, 1H, NH), 4.70 - 4.61 (m, 2H, 2 × CH), 4.00 – 3.89 (m, 12H, 6 × OCH_2), 1.81 – 0.86 (m, 120H, 48 × CH_2, 8 × CH_3,); MS (FAB^+): *m/z* calcd. for $C_{79}H_{141}N_3O_9$: 1276.1; found: 1275.7; elemental anaylsis calcd (%) for $C_{79}H_{141}N_3O_9$: C 74.30, H 11.13, N 3.29; found: C 73.91, H 11.34, N 3.17.

3b : R_f = 0.69 in 40% EtOAc-hexanes; a white solid; yield: 70 %; IR (KBr pellet): ν = 3273, 2922, 2865, 1628, 1580 cm^{-1}; $[\alpha]_D^{25}$ = +19.15 (c = 1 in $CHCl_3$); UV/Vis: λ_{max} = 263.39 nm, ∈ = 21.11 × 10^3 L $mol^{-1}cm^{-1}$; ^{1}H NMR (400MHz, $CDCl_3$): δ 8.19 (s, 1H, NH), 6.96 (s, 2H, Ar), 6.88 (s, 2H, Ar), 6.75 (d, J = 6.2, 1H, NH), 6.51 (d, J = 6.4, 1H, NH) 4.63 - 4.58 (m, 2H, 2 × CH), 4.08 - 3.83 (m, 12H, 6 × OCH_2), 1.81 – 0.86 (m, 120H, 48 × CH_2, 8× CH_3); ^{13}C NMR (100MHz, $CDCl_3$): 172.60, 169.84, 167.57, 153.20, 153.12, 141.77, 134.85, 133.45, 128.11, 105.85, 98.79, 73.53, 73.46, 69.42, 69.03, 49.80, 31.90, 30.32, 29.72, 29.64, 29.60, 29.44, 29.38, 29.35, 26.10, 22.67, 18.22, 17.66, 14.01; MS (FAB^+): *m/z* for calcd. $C_{79}H_{141}N_3O_9$: 1276.1; found: 1276.7; elemental anaylsis calcd (%) for $C_{79}H_{141}N_3O_9$: C 74.30; H 11.13, N 3.29; found: C 74.45, H 11.42, N 3.20.

3c :R_f = 0.67 in 40% EtOAc-hexanes; yield: 70%; IR (KBr pellet): ν = 3288, 2922, 2851, 1625 and 1582 cm^{-1}; $[\alpha]_D^{26}$ = +1.5 (*c* = 1 in $CHCl_3$); UV/ViS: λ_{max} = 261.24 nm, ∈ = 21.55 × 10^3 L $mol^{-1}cm^{-1}$; ^{1}H NMR (400MHz, $CDCl_3$): δ 8.43 (s, 1H, NH), 6.95 (s, 2H, Ar), 6.89 (s, 2H, Ar), 6.66 (d, *J* = 6.2, 1H, NH), 6.49 (d, *J* = 6.4, 1H, NH), 4. 63 - 4.46 (m, 2H, 2 × CH), 3.98 – 3.78 (m, 12H, OCH_2 × 6), 1.79 – 0.85 (m, 120H, 48 × CH_2, 8 × CH_3); ^{13}C NMR (400MHz, $CDCl_3$): 172.62, 169.78, 168.04, 153.35, 153.23, 142.33, 133.44, 128.23, 106.43, 104.08, 99.76, 73.59, 69.74, 69.36, 50.25, 49.96, 31.93, 30.41, 29.65, 29.51, 29.35, 26.16, 22.65, 17.82, 17.70, 13.10; MS (FAB^+): *m/z* for calcd. $C_{79}H_{141}N_3O_9$: 1276.1; found: 1275.8; elemental anaylsis calcd (%) for $C_{79}H_{141}N_3O_9$: C 74.30, H 11.13, N 3.29; found: C 74.04, H 11.13, N 3.18.

4a : R_f = 0.80 in 20% EtOAc-hexanes; yield: 72%; IR (KBr pellet): ν = 3264, 2924, 2853, 1630, 1578, 1549 cm^{-1}; $[\alpha]_D^{26}$ = -10.63 (*c* = 1 in $CHCl_3$); UV/Vis: λ_{max} = 264.79 nm, ∈ = 26.36 × 10^3 L $mol^{-1}cm^{-1}$; ^{1}H NMR (400MHz, $CDCl_3$): δ 8.26 (s, 1H, NH), 6.95 (s, 2H, Ar), 6.86 (s, 2H, Ar), 6.81 (d, *J* = 6.6, 1H, NH), 6.52 (d, *J* = 5.4, 1H, NH), 4.66 (m, 1H, CH), 4.55 (m, 1H, CH), 3.97 – 3.88 (m, 12H, 6 × OCH_2), 1.78 – 0.86 (m, 132H, 2 × CH, 50 × CH_2, 10 × CH_3); MS (FAB^+): *m/z* for calcd. $C_{85}H_{153}N_3O_9$: 1360.2; found: 1360.5; elemental anaylsis calcd (%) for $C_{85}H_{153}N_3O_9$: C 75.00, H 11.33, N 3.09; found: C 75.29, H 11.55; N 3.23.

4b : R_f = 0.80 in 20% EtOAc-hexanes; yield: 71%; IR (KBr pellet): ν = 3263, 2924, 2853, 1631, 1580, 1504 cm^{-1}; $[\alpha]_D^{26}$ = +11.0 (*c* = 1 in $CHCl_3$); UV/Vis: λ_{max} = 263.78 nm, ∈ = 22.83 × 10^3 L $mol^{-1}cm^{-1}$; ^{1}H NMR (400MHz, $CDCl_3$): δ 8.23 (s, 1H, NH), 6.94 (s, 2H, Ar), 6.87 (s, 2H, Ar), 6.73 (d, *J* = 6.6, 1H, NH), 6.43 (d, *J* = 5.4, 1H, NH), 4.51 (m, 1H, CH), 4.53 (m, 1H, CH), 3.97 – 3.88 (m, 12H, 6 × OCH_2), 1.79 – 0.86 (m, 132H, 10 × CH_3, 50 × CH_2, 2 × CH); ^{13}C NMR (400MHz, $CDCl_3$): 172.64, 169.73, 167.67, 153.38, 153.30, 142.39, 133.50, 128.27, 106.44, 99.36, 73.61, 73.53, 69.76, 69.33, 52.87, 52.68, 40.92, 40.51, 31.92, 30.39, 29.64, 29.51, 29.34, 26.14, 25.15, 24.94, 22.88, 22.65, 22.20, 21.10, 14.00; MS (FAB^+): *m/z* for calcd. $C_{85}H_{153}N_3O_9$: 1360.2; found: 1359.74; elemental anaylsis calcd (%) for $C_{85}H_{153}N_3O_9$: C 75.00, H 11.33, N 3.09; found: C 74.94, H 11.50, N 3.22.

4c : R_f = 0.74 in 20% EtOAc-hexane; a white solid; yield: 74%; IR (KBr pellet): ν = 3289, 2923, 2853, 1633 1612 cm^{-1}; $[\alpha]_D^{26}$ = +1.18 (*c* = 1 in $CHCl_3$); UV/Vis: λ_{max} = 261.80 nm, ∈ = 25.51 × 10^3 L $mol^{-1}cm^{-1}$; ^{1}H NMR (400MHz, CDCl3): δ 8.45 (s, 1H, NH), 6.97 (s, 2H, Ar), 6.87 (s, 2H, Ar), 6.43 (d, *J* = 6.6, 1H, NH), 6.33 (d, *J* = 5.4, 1H, NH), 4.60 (m, 1H, CH), 4.43 (m, 1H, CH), 3.97 – 3.83 (m, 12H,

OCH_2 × 6), 1.78 – 0.85 (m, 132H, 2 × CH, 50 × CH_2, 10 × CH_3); MS (FAB^+): *m/z* for calcd. $C_{85}H_{153}N_3O_9$: 1360.2; found: 1359.7; elemental anaylsis calcd (%) for $C_{85}H_{153}N_3O_9$: C 75.00, H 11.33, N 3.09; found: C 74.80, H 11.48, N 3.21.

III. ^{1}H-^{1}H COSY NMR Profile

As a representative case ^{1}H-^{1}H COSY NMR spectrum was obtained for the compound **3b** (see below Fig. S1) The profile clearly elucidate that NH protons appearing as two doublets (centered at about δ 7.2 and 6.8) couple with methine proton (occurring as two multiplets centered at about δ 4.72 and 4.6) of peptide chain that convincingly support the structure of the compound.

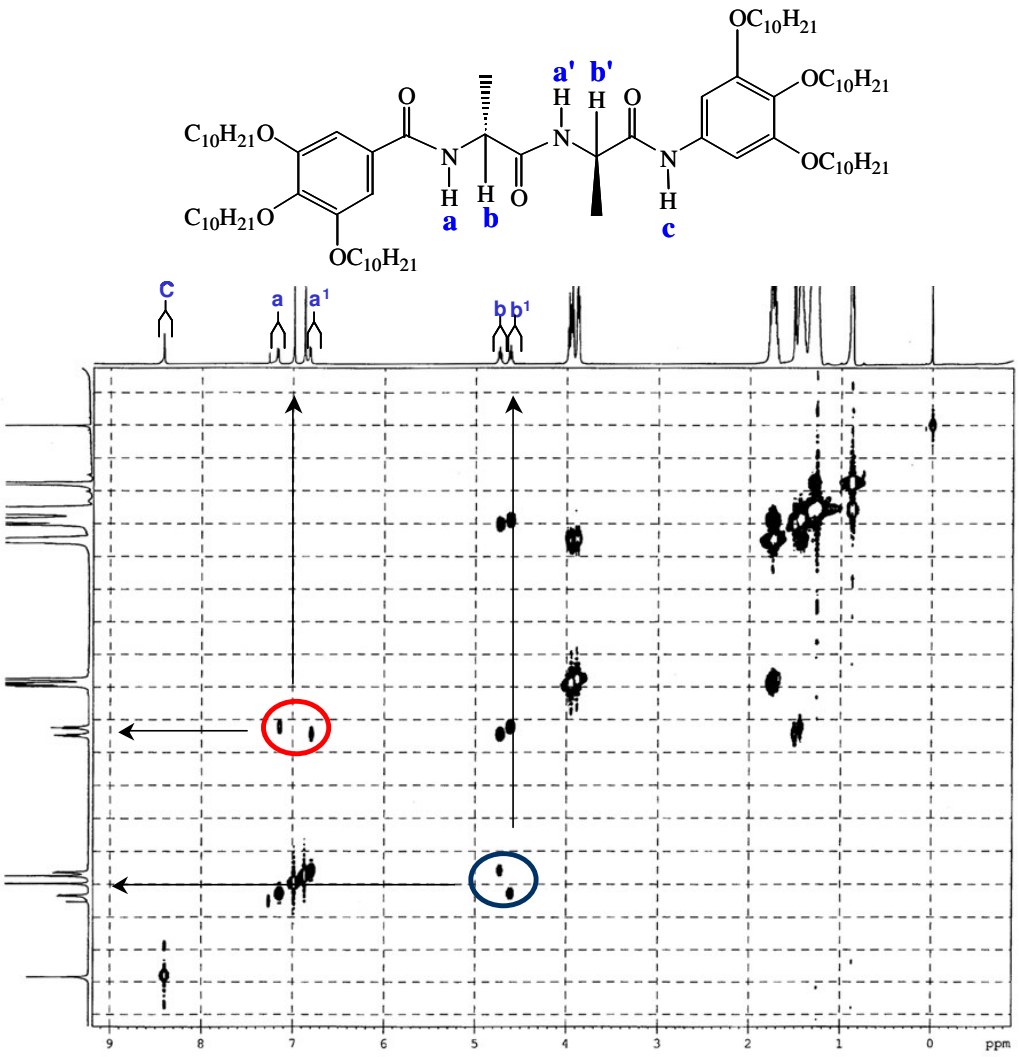

Figure S1: ^{1}H-^{1}H COSY NMR spectrum of peptide **3b**.

IV. Differential scanning calorimetric studies

Figures S2 shows DSC traces obtained for the dipeptides **3b** during the repetitive heating and cooling cycles. The Col_{ob} phase once formed upon melting the crystalline sample, does not crystallize as evidenced by the fact that, no exothermic (from just below the Col_{ob} to -60 ^{o}C) or endothermic (from -60 ^{o}C to near the Col-Iso phase transition) peaks were seen in the first cooling or second heating DSC profiles respectively. Thus Col phase occurs for very wide thermal range.

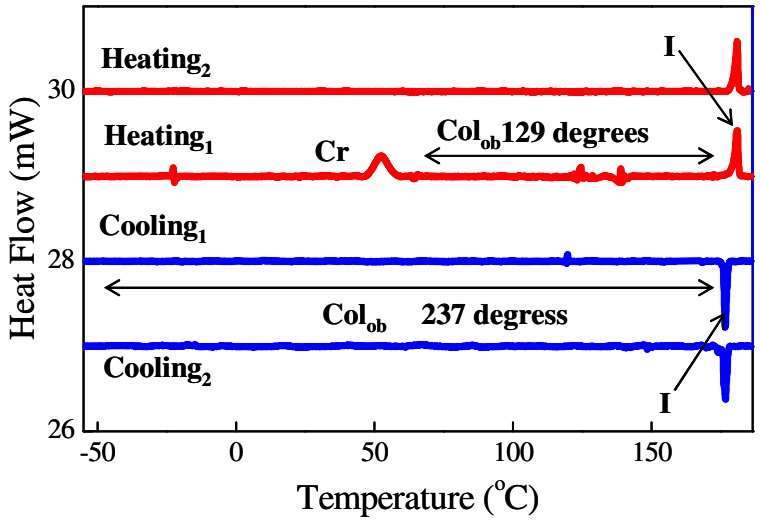

Figure S2: DSC profiles recorded, during the first heating - cooling and second heating and cooling cycles, for compound **3b**. Notice that the Col_{ob} phase exists for a very wide thermal range and mesophase does not reverts to solid state once melted.

V. FTIR Spectra

The FTIR data provided the evidence for the existence of intermolecular hydrogen bonding in solid state as well as in their mesophase. For quantitative analysis, samples (about 1 mg) were sandwiched between the KBr cells and FTIR was recorded as a function of temperature with the help of a hot stage. It was found that the ν(N-H), ν(C=O) bands become stronger (increase in the intensity) which is pronounced near room temperature, indicating that all the NH and C=O are involved in the hydrogen bonding in their solid states as well as mesophases. As a representative case, the FTIR traces obtained during the cooling process from the isotropic phase at different temperature for ν(N-H) and ν(C=O) bands are shown in Fig. S3

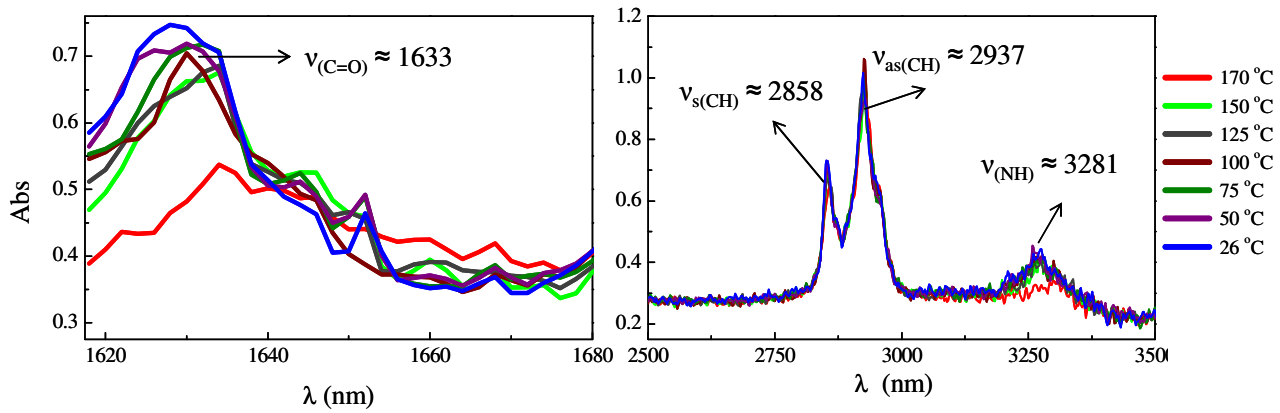

Figure S3: FTIR spectra obtained during cooling the sample **3a** from its isotropic phase. Notice that the intensity of peak keep increasing with decrease in temperature with a small shift in the peak position.

VI. CD Spectra

The circularly dichroic (CD) spectroscopy measurement carried out at 23 ^{o}C on the dilute solutions, all the dipeptides (1 mg in 1 ml of CH_2Cl_2; Cell length = 1mm) showed a significant cotton effect indicating that the molecules self-assemble into helical array through the H-bonding. For example, the pairs of enantiomeric peptides **4a**-**4b** (see Figure. S4A) **3a**-**3b** (see Figure. S4B) and as anticipated, exhibit mirror image cotton effect. Similarly for the dipeptide **4c** (Figure S4C) and **3c** (Figure S4D)**,** CD spectra were obtained for their solution for the above mentioned concentration. In order to examine the nature of the fluid columnar (Col) aggregates formed by the enantiomeric pair dipeptides **3a-b** and **4a-b**, Optical measurement was carried out, (1 mg of the sample placed in a quartz cell) with the aid of circularly dichroic (CD) spectroscopy, in the entire temperature range of the mesophase. The CD patterns obtained for the compounds **3a**, **3b** and **4b, 4a** have been shown in Figures S4E, S4F, S4G and S4H respectively. The fact that Cotton effect is observed in the Col phase, establishes that the structural organization is due to intermolecular H-bonding between the hexacatenar like mesogens within the same column causing a helical array directed by stereochemistry of peptide chain and their intermolecular interactions.

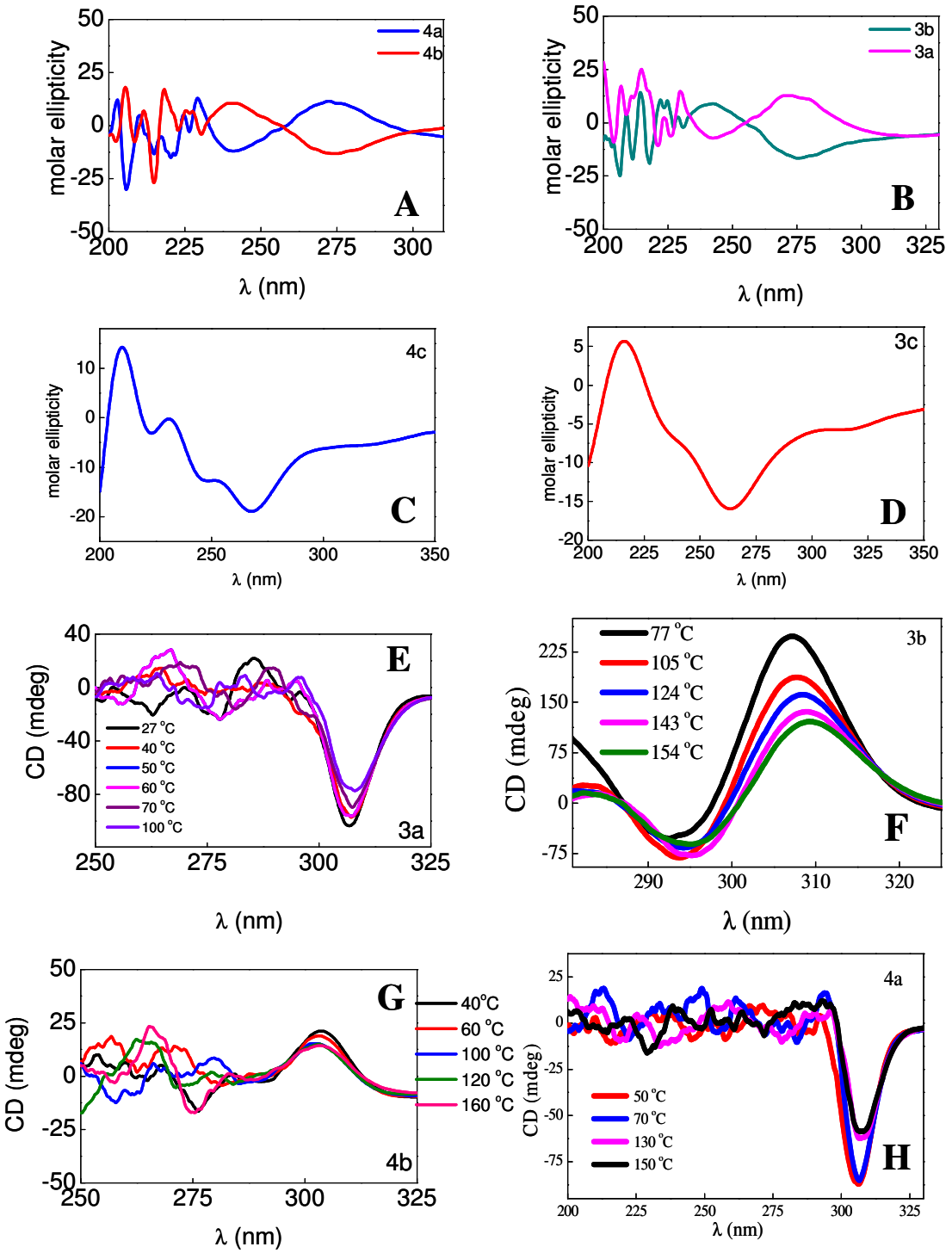

Figure S4: CD spectra of dipeptides **4a-b** (A), **3a-b** (B), **4c** (C) and **3c** (D) for their dilute solutions. Also shown the CD patterns obtained at different temperatures of the columnar phase formed by the compounds **3a**, (E), **3b** (F);**4b** (G) and **4a** (H). Notice that, these columnar structures exhibit Cotton Effect.

VII. X-ray diffraction study

The structure of the Col phases was investigated with the help of powder X-ray diffraction studies. **Fig**. **S5A, S5B**, **S5C**, **S5D** and **S5E**, show the 2D-pattern as well as 1D profiles obtained for samples of **3a**, **3b**, **3c, 4b** and **4c** respectively.

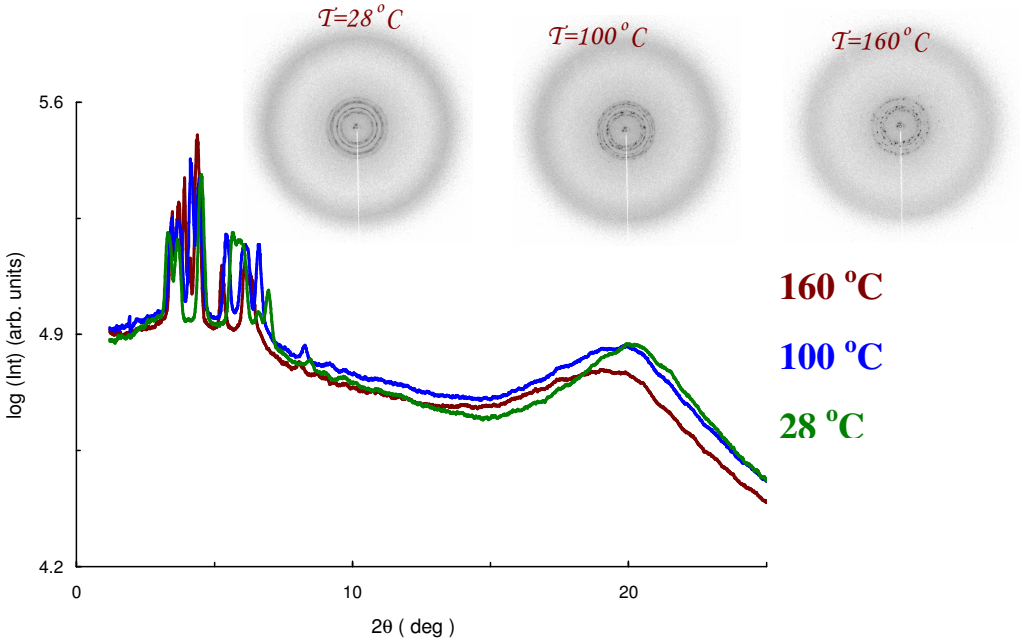

Figure S5A: 1D-Intensity against 2θ (bottom) profile derived from 2D-XRD pattern (see top pictures) for the sample **3a** at different temperatures. Notice that all the diffraction patterns look nearly identical.

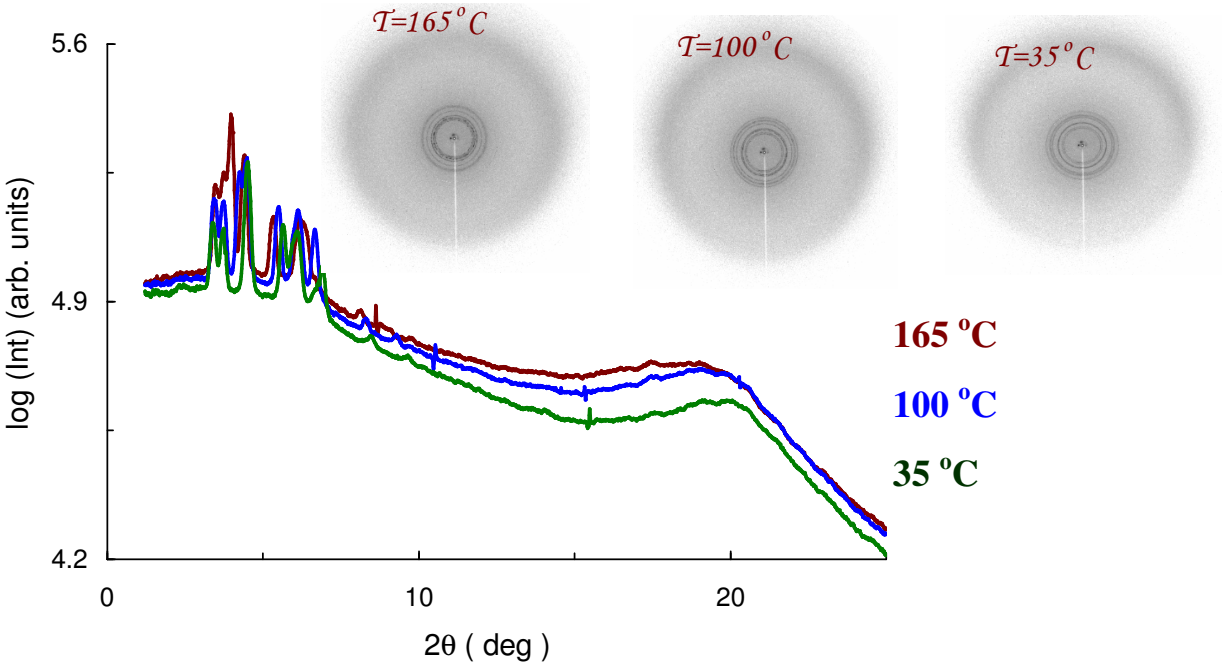

Figure S5B: 1D-Intensity *vs* 2θ (bottom) profile derived from 2D-XRD pattern (see top pictures) for the sample **3b** at different temperatures. Seemingly, the profiles are almost similar to the one obtained for **3a**.

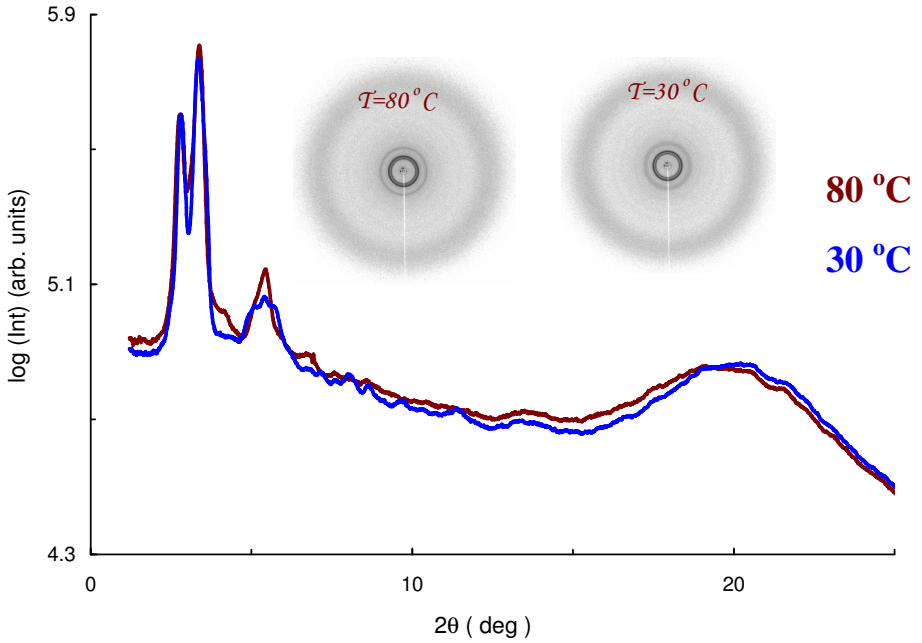

Figure S5C: 1D-Intensity *vs* 2θ (bottom) profile derived from 2D-XRD pattern (see top patterns) for the sample **3c** at two different temperatures.

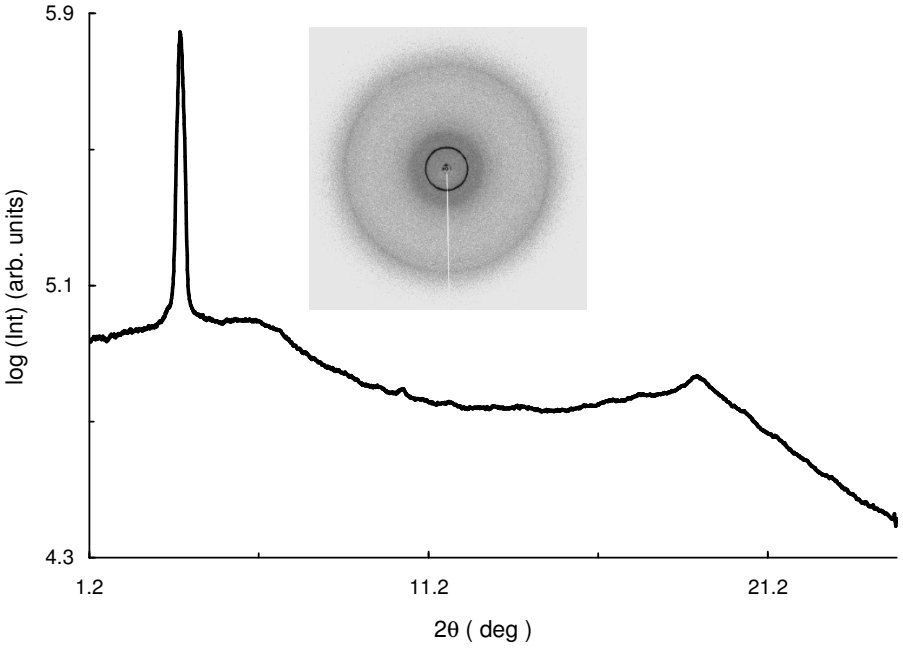

Figure S5D: 1D-Intensity *vs* 2θ profile derived from 2D-XRD pattern of Col phase of compound **4b** at 210 ^{o}C.

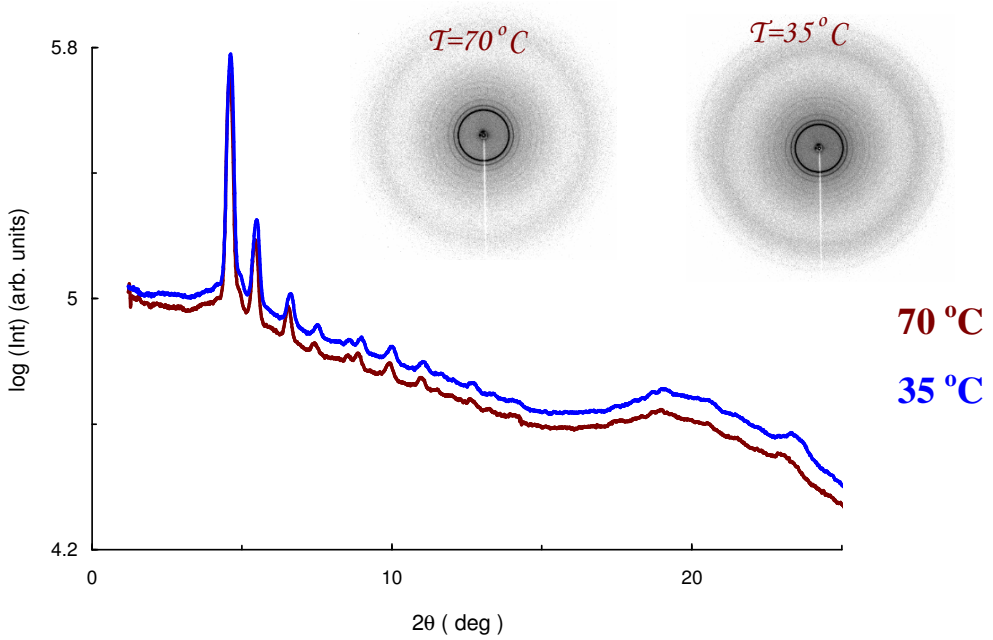

Figure S5E: 1D-Intensity *vs* 2θ profile derived from 2D-XRD pattern of the Col_r phase of the dipeptide **4c** at two different temperatures.

X-ray data of homomeric dipeptides at different temperatures

Dipeptides	T / °C	Phase	*d* obsd (Å)	*d calcd* (Å)	Miller index	Lattice parameters (Å)
4c	35	Col_r	19.14 16.12 13.35 11.75 10.30 9.84 8.84 8.01 7.59 6.97 6.61 4.48 3.80	19.05 16.10 13.31 11.82 10.73 9.77 9.53 7.95 7.65 7.08 6.35	110 200 210 020 300 310 220 320 130 230 330	a = 32.2 b = 23.6
3c	35	Col_r	31.45 26.30 16.25 4.38	31.45 26.31 16.01	110 200 310	a = 52.6 b = 39.2

VIII. CD spectra of gel

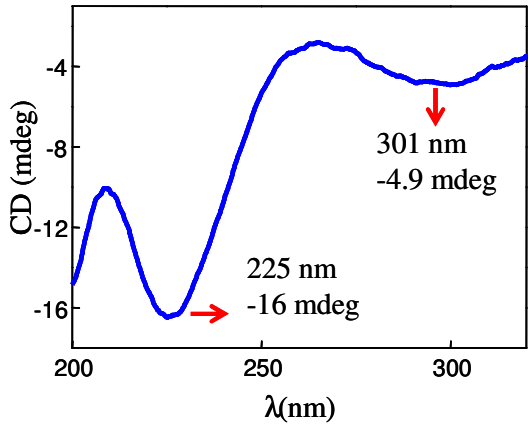

Figure S6: CD spectra of gel in ethanol 5% (w/v) obtained at room temperature, exhibits cotton effects.

IX. Scanning electron microscopy (SEM) images.

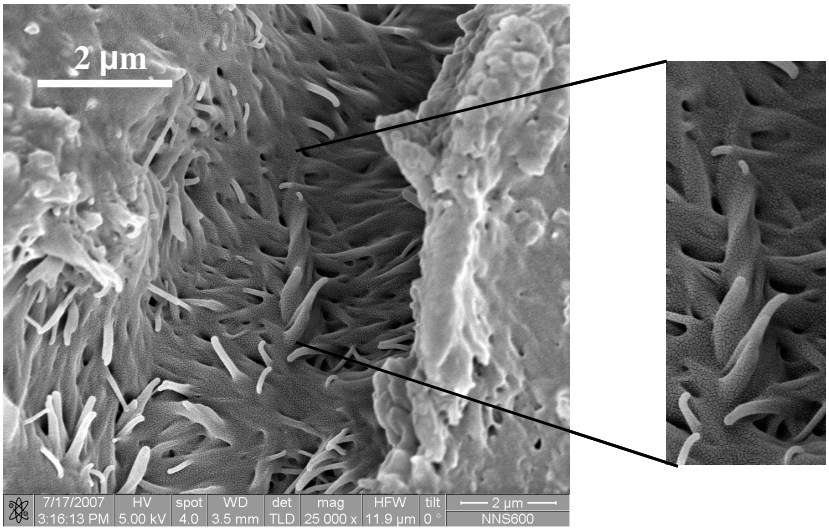

Figure S7: SEM images of the dipeptide **3b** obtained at the room temperature.